DOI: 10.24996/ijs.2022.63.9.23

ISSN: 0067-2904

# Study of the Impact of Unsteady Squeezing Magnetohydrodynamics Copper-Water with Injection-Suction on Nanofluid Flow Between Two Parallel Plates in Porous Medium

**Abeer Majeed Jasim**

*Department of Mathematics, College of Science, University of Basrah,Basrah, Iraq*

Received: 13/10/2021 Accepted: 9/12/2021 Published: 30/9/2022

**Abstract**

In this article, the existence of thermal radiation with Copper- water nanofluid, the effect of heat transfer in unsteady magnetohydrodynamics (MHD) squeezing and suction-injection on the flow between parallel plates( porous medium) are studied. Rosseland approximation and the radiation of heat flux are used to depict the energy equation. The set of ordinary differential equations with boundary conditions are analytically resolved by applying a new approach method (NAM). The influences of thermal field and physical parameters on dimensionless flow field have been displayed in tabular and graphs form. The presented results show that the heat transfer coefficient is reduced by the thermal radiation coefficient increases and the absolute values of the skin friction coefficients are enhanced with the magnetic amplification parameter. Regularly, the present outcomes discern that the parameters of the injection-suction coefficient are both the temperature and velocity profiles decline.

**Keyword:** Thermal radiation, Copper nanofluid, Magnetohydrodynamics, Parallel plates, Porous medium.

# دراسة تأثير الضغط غير المستقر للديناميكا المائية والماء النحاسي مع الحقن– الشفط على تدفق السوائل النانوية بين لوحين متوازيين في وسط مسامي

**عبير مجيد جاسم**

قسم الرياضيات، كلية العلوم ، جامعة البصرة ، البصرة، العراق

**الخلاصة**

في هذا البحث ، في حالة وجود إشعاع حراري مع النحاس – السائل النانوي المائي ، تمت دراسة تأثير انتقال الحرارة في الديناميكا المائية المغناطيسية غير المستقرة والضغط والحقن–الشفط على التدفق بين الصفائح المتوازية (وسط مسامي). يتم استخدام تقريب روسلاند وإشعاع تدفق الحرارة لتصوير معادلة الطاقة. تم حل مجموعة المعادلات التفاضلية العادية بشروط حدية تحليليًا عن طريق تطبيق تقنية تعرف طريقة نهج جديدة . كذلك تم عرض معاملات تأثير المجال الحراري والفيزيائي على مجال التدفق بلا أبعاد في شكل جداول ورسوم بيانية. تم عرض تأثيرات المجال الحراري والمعلمات الفيزيائية على مجال التدفق بلا أبعاد في شكل جداول ورسوم بيانية. أظهرت النتائج التي تم الحصول عليها أن معامل انتقال الحرارة ينخفض بزيادة معامل الإشعاع الحراري ، كما أن القيم المطلقة لمعاملات احتكاك الجلد تتعزز بمعامل تضخيم مغناطيسي.

*Email: abeer.jassem@yahoo.com

بشكل منتظم ، تبين النتائج الحالية أن معاملات معامل شفط– الحقن هي كل من انخفاض درجات الحرارة والسرعة.

## 1.Introduction

During the past decade, in many branches of science and engineering, there are many applications of analysis for heat and mass transfer such as from stains to the environment water is evaporated, and within the liver and kidneys the blood is sterilized which are related to mass transfer applications. For the heat transfer, it includes evaporators and the field of condensers. The rate of mass and heat transfer has a legacy of much use, as lubrication method, polymer dispensation, chemical dispensation equipment, fog formation and dispersion, because of the frosty spoils on the crops, Azimin and Riazi [1] studied the impact of the heat transfer for GO-water nanofluid between two analogous disks. They found that an increase in the values of the Brownian number leads to increase volume concentration of nanoparticle. During a vertical porous channel via convective heat source for nanofluid on MHD flow, Das et al. [2] have examined the influence of entropy exploration. In the porous medium, Aziz et al. [3] have analyzed the effect of free convection on nanofluid past plate implanted a smooth plane and in the happening of gyrotactic microorganisms increasing the value of bio-convection parameters rate of mass transfer, Nusselt number and motile density parameter enhanced, while it decreases with growing the values of buoyancy parameter *Nr*. Domairry and Hatami [4] have studied numerical investigation of squeezing flow through similar plates with Copper–water nanofluid with a raising the values of volume fraction of solid particle, there is no change in velocity boundary layer depth. Through a porous medium inside a square cavity packed in nanofluids, Grosan et al. [5] exaimed the free convection effect of heat transfer. Through a channel with porous walls, Fakour et al. [6] deliberated the impact of a nanofluids flow of magnetohydrodynamic and heat conduction. Gupta and Ray [7] have discussed a numerical analysis of the squeezing nanofluid flow among two similar plates and they proved that as the temperature of the nanoparticle increases with increase in Prandtl number and Eckert number. In this paper, we study the effects associated with MHD flow of heat transfer. Before being solved, similarity solution is used to convert the governing partial differential equations into ordinary differential equations using NAM. The effects of different physical numbers on the flow and the thermal profiles are analyzed. Therefore, the organizations of this paper are:

- In order to reveal the behaviour fluid flow and of heat transfer with thermal radiation for Copper-water nanofluid.
- We simulate the behaviour of the pertinent parameters such as porous medium, thermal raditian, injection-susjection, solid volume fraction, Eckert number, Prandtl number and the length parameter on the curves of the fluid flow and temperature distributions. We alos examine the graphical of the parameters on the velocity and the temperature distributions.
- We use NAM with similarity transformations to understand the behavior of the heat transfer. An approximate analytical solution from the proposed method could be established mathematical formulations to describe different microfluidic devices.
- The point of the current study is to find approximate analytical solutions and to analyze the influence of suction- injection and thermal radiation on unsteady MHD squeezing Copper-water nanofluids flow between similar plates in the presence of porous medium. Obtained equations have been solved by new approach technique with assisent the initial and boundary conditions and compared with DTM[4] and 4-5th Runge-Kutta-Fehlberg technique [8]. Through the graphs, the effect is described various objective parameters on speed and temperature fields.

## 2. Problem Statement

In the porous medium, nanofluid flow unsteady two-dimensional squeezing between two similar plates in the presence of the thermal radiatio with suction - injection is considered.

$\tilde{y} = (1 - \bar{\alpha}\tilde{t})^{0.5} = \pm\tilde{h}(\tilde{t})$ is the space between two plates. There are two cases for convergent both the plates in the following:

- Both plates are compact units to which they are connected for $\bar{\alpha} > 0$ and $\tilde{t} = \frac{1}{\bar{\alpha}}$.
- The two plates are separated for $\bar{\alpha} < 0$.

The physical model graph along with the coordinate system and flow pattern is defined in Figure (1):

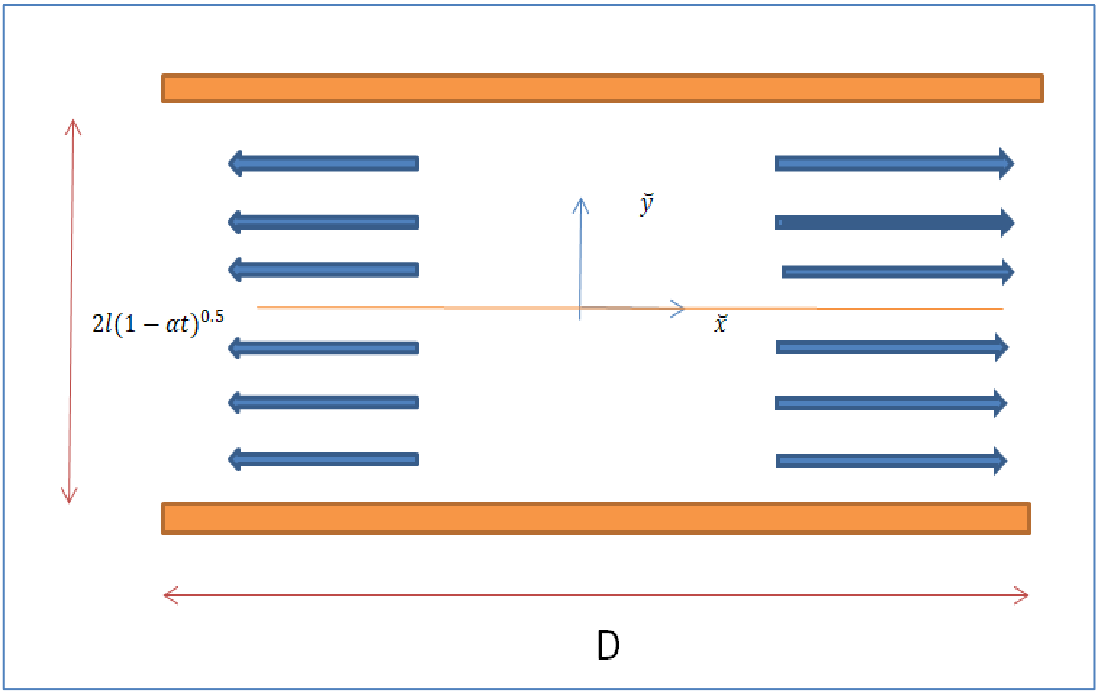


**Figure 1-**Coordinate System and Flow Configuration.

The basic equations for the mass, momentum, and heat transfer of the nanofluid are expressed

$$\frac{\partial \tilde{u}}{\partial \tilde{x}} + \frac{\partial \tilde{v}}{\partial \tilde{y}} = 0, \tag{2.1a}$$

$$\tilde{\rho}_{nf}\left(\frac{\partial \tilde{u}}{\partial \tilde{t}} + \tilde{u}\frac{\partial \tilde{u}}{\partial \tilde{x}} + \tilde{v}\frac{\partial \tilde{u}}{\partial \tilde{y}}\right) = -\frac{\partial \tilde{p}}{\partial \tilde{x}} + \tilde{\mu}_{nf}\left(\frac{\partial^2 \tilde{u}}{\partial \tilde{x}^2} + \frac{\partial^2 \tilde{u}}{\partial \tilde{y}^2}\right) - \frac{\nu\tilde{\rho}_{nf}}{\tilde{k}}\tilde{u} - \tilde{\sigma}A_0\tilde{u}, \tag{2.1b}$$

$$\tilde{\rho}_{nf}\left(\frac{\partial \tilde{v}}{\partial \tilde{t}} + \tilde{u}\frac{\partial \tilde{v}}{\partial \tilde{x}} + \tilde{v}\frac{\partial \tilde{v}}{\partial \tilde{y}}\right) = -\frac{\partial \tilde{p}}{\partial \tilde{y}} + \tilde{\mu}_{nf}\left(\frac{\partial^2 \tilde{v}}{\partial \tilde{x}^2} + \frac{\partial^2 \tilde{v}}{\partial \tilde{y}^2}\right) - \frac{\nu\tilde{\rho}_{nf}}{\tilde{k}}\tilde{v} - \tilde{\sigma}A_0\tilde{v}, \tag{2.1c}$$

$$\frac{\partial \tilde{T}}{\partial \tilde{t}} + \tilde{u}\frac{\partial \tilde{T}}{\partial \tilde{x}} + \tilde{v}\frac{\partial \tilde{T}}{\partial \tilde{y}} = \frac{\tilde{k}_{nf}}{(\tilde{\rho}\,\tilde{c}_p)_{nf}}\left(\frac{\partial^2 \tilde{T}}{\partial \tilde{x}^2} + \frac{\partial^2 \tilde{T}}{\partial \tilde{y}^2}\right) + \frac{\tilde{\mu}_{nf}}{(\tilde{\rho}\,\tilde{c}_p)_{nf}}\left(4\left(\frac{\partial \tilde{u}}{\partial \tilde{x}}\right)^2 + \left(\frac{\partial \tilde{u}}{\partial \tilde{y}} + \frac{\partial \tilde{v}}{\partial \tilde{x}}\right)^2\right) - \frac{1}{(\tilde{\rho}\,\tilde{c}_p)_{nf}}\frac{\partial \tilde{q}_r}{\partial \tilde{y}}, \tag{2.1d}$$

for radiation, the heat flux by using Rosseland approximation [4] defined as:

$$\tilde{q}_r = -\frac{4\tilde{\sigma}}{3\tilde{k}}\frac{\partial \tilde{T}^4}{\partial \tilde{y}}, \tag{2.1f}$$

Thus, we assume that the deviation of the temperature within the flow is to expedite $\tilde{T}^4$ stretching in the Taylor series and growing $\tilde{T}^4$ about $\tilde{T}_\infty$ and the higher order of deserting terms, yield:

$$\frac{\partial \tilde{T}}{\partial \tilde{t}} + \tilde{u}\frac{\partial \tilde{T}}{\partial \tilde{x}} + \tilde{v}\frac{\partial \tilde{T}}{\partial \tilde{y}} = \frac{\tilde{k}_{nf}}{(\tilde{\rho}\,\tilde{c}_p)_{nf}}\frac{\partial^2 \tilde{T}}{\partial \tilde{x}^2} + \frac{\tilde{k}_{nf}}{(\tilde{\rho}\,\tilde{c}_p)_{nf}}\left(1 + \frac{16\tilde{\sigma}\tilde{T}_\infty^3}{3\tilde{k}\tilde{k}_{nf}}\right)\frac{\partial^2 \tilde{T}}{\partial \tilde{y}^2} + \frac{\tilde{\mu}_{nf}}{(\tilde{\rho}\,\tilde{c}_p)_{nf}}\left(4\left(\frac{\partial \tilde{u}}{\partial \tilde{x}}\right)^2 + \left(\frac{\partial \tilde{u}}{\partial \tilde{y}} + \frac{\partial \tilde{v}}{\partial \tilde{x}}\right)^2\right), \tag{2.1d}$$

where $\tilde{x}$ and $\tilde{y}$ direction velocity components are $(\tilde{u}, \tilde{v})$ correspondingly, $\tilde{\sigma}$ is the Stefan Boltzmann fixed, $\tilde{k}$ is coefficient of mean absorption, $\tilde{\mu}_{nf}$ is dynamic viscosity, $\tilde{\rho}_{nf}$ is density, $\tilde{k}_{nf}$ is thermal conductivity, and $(\tilde{\rho}\,\tilde{C}_p)_{nf}$ is heat capacity. The boundary condition are defined as follows:

$$\tilde{u} = 0, \quad \tilde{v} = V_w(\tilde{x}, \tilde{t}), \; \tilde{T} = \tilde{T}_H \quad \text{at} \quad \tilde{y} = \tilde{h}(\tilde{t}), \tag{2.2a}$$

$$\frac{\partial \tilde{u}}{\partial \tilde{y}} = 0, \; \tilde{v} = -\frac{\bar{\alpha}\,\tilde{t}}{2(1-2\bar{\alpha}\,\tilde{t})^{0.5}}\, e_w, \; \frac{\partial \tilde{T}}{\partial \tilde{y}} = 0 \; \text{at} \; \tilde{y} = 0. \tag{2.2b}$$

Now, the parameter $e_w$ appears in three cases as it is shown

- If $e_w > 0$, then $e_w$ is the suction parameter.
- If $e_w = 0$, then the fixd surface.
- If $e_w < 0$, then $e_w$ is the injection parameter.

The effective of $\tilde{\mu}_{nf}$, $\tilde{\rho}_{nf}$, $\tilde{k}_{nf}$, and $(\tilde{\rho}\,\tilde{C}_p)_{nf}$ can be written respectively as:

$$\tilde{\mu}_{nf} = \frac{\tilde{\mu}_f}{(1-\omega)^{2.5}}, \tag{2.3a}$$

$$\tilde{\rho}_{nf} = (1-\omega)\tilde{\rho}_f + \omega\tilde{\rho}_s, \tag{2.3b}$$

$$(\tilde{\rho}\,\tilde{C}_p)_{nf} = (1-\omega)(\tilde{\rho}\,\tilde{C}_p)_f + \omega(\tilde{\rho}\,\tilde{C}_p)_s, \tag{2.3c}$$

$$\frac{\tilde{k}_{nf}}{\tilde{k}_f} = \frac{\tilde{k}_s + 2\tilde{k}_f - 2\omega(\tilde{k}_f - \tilde{k}_s)}{\tilde{k}_s + 2\tilde{k}_f + 2\omega(\tilde{k}_f - \tilde{k}_s)}, \tag{2.3d}$$

where $\omega$ is solid volume fraction, $s$ is solid particle and $f$ is the regular fluid. The thermo physical properties of water and copper are offered in Table (1):

**Table 1-** Density properties of nanofluids and nanoparticles

| **Material** | **Density (kg/m$^3$)** | **Thermal conductivity (W/mk)** | **Heat capacity(j/kgK)** |
|---|---|---|---|
| Copper $Cu$ | 8933 | 0.613 | 4179 |
| Fluid phase (water) | 997.1 | 401 | 385 |

Equations (2.1a)-(2.1d) can be transfered into the ordinary differential equations by means of the following similarity variables:

$$\xi = \frac{\tilde{u}}{l(1-\bar{\alpha}\tilde{t})^{1/2}}, \; \tilde{u} = \frac{\bar{\alpha}}{2(1-\bar{\alpha}\,t)}\frac{dg(\xi)}{d\xi}, \; \tilde{v} = -\frac{\bar{\alpha}\,l}{2(1-\bar{\alpha}\,\tilde{t})}g(\xi), \; \theta = \frac{\tilde{T}}{\tilde{T}_H}, \tag{2.4}$$

The modified ordinary differential equations are:

$$\frac{d^4g}{d\xi^4} - SB_1(1-\omega)^{0.5}\left(\xi\frac{d^3g}{d\xi^3} + 3\frac{d^2g}{d\xi^2} + \frac{dg}{d\xi}\frac{d^2g}{d\xi^2} - g\frac{d^3g}{d\xi^3}\right) - (\gamma + M)\frac{d^2g}{d\xi^2} = 0, \tag{2.5a}$$

$$(1+N_r)\frac{d^2\theta}{d\xi^2} + \frac{B_2}{B_3}P_rS\left(g\frac{d\theta}{d\xi} - \xi\frac{d\theta}{d\xi}\right) + \frac{P_rE_c}{B_3(1-\omega)^{2.5}}\left[\left(\frac{d^2g}{d\xi^2}\right)^2 + 4\delta^2\left(\frac{dg}{d\xi}\right)^2\right] = 0, \tag{2.5b}$$

with the boundary conditions become

$$g(0) = e_w, \; \frac{d^2g(0)}{d\xi^2} = 0, \; \frac{d\theta(0)}{d\xi} = 0, \quad \text{at} \; \xi = 0, \tag{2.6a}$$

$$g(1) = 1, \; \frac{dg(1)}{d\xi} = 1, \; \theta(1) = 1, \; \text{at} \; \xi = 1, \tag{2.6b}$$

Now, we can define the physical parameter as:

- The squeeze parameter is $S = \frac{\bar{\alpha}l^2}{2\nu_f}$,
- The Eckert parameter is $E_c = \frac{\tilde{\rho}_f}{(\tilde{\rho}\,\tilde{C}_p)_f}\left(\frac{\bar{\alpha}\tilde{x}}{2(1-2\bar{\alpha}\tilde{t})}\right)^2$,
- The Prandtl parameter is $P_r = \frac{\tilde{\mu}_f(\tilde{\rho}\,\tilde{C}_p)_f}{\tilde{\rho}_f\tilde{k}_f}$,
- The thermal radiation parameter is $N_r = \frac{16\tilde{\sigma}\tilde{T}_\infty^3}{3\tilde{k}\tilde{k}_{nf}}$,

- The porous medium is $\gamma = \frac{2l^2 \nu(1-\bar{\alpha}\tilde{t})}{\tilde{k}\tilde{\mu}_{nf}}$,
- The magnetic parameter is $M = \frac{2l^2 \tilde{\sigma} A_0^2 (1-\bar{\alpha}\tilde{t})}{\tilde{\rho}\tilde{\mu}_{nf}}$
- The length parameter is $\delta = \frac{1}{\tilde{x}}$,
- The suction - injection parameter is $e_w = -\frac{2(1-\bar{\alpha}\tilde{t})^{0.5} V_w(\tilde{x})}{\bar{\alpha} l}$,
- $B_1 = (1-\omega) + \omega \frac{\tilde{\rho}_s}{\tilde{\rho}_f}$, $B_2 = (1-\omega) + \omega \frac{(\tilde{\rho}\,\tilde{C}_p)_s}{(\tilde{\rho}\,\tilde{C}_p)_f}$, $B_3 = \frac{\tilde{k}_{nf}}{\tilde{k}_f} = \frac{\tilde{k}_s + 2\tilde{k}_f - 2\omega(\tilde{k}_f - \tilde{k}_s)}{\tilde{k}_s + 2\tilde{k}_f + 2\omega(\tilde{k}_f - \tilde{k}_s)}$ are

constants.

For the particle interest, the coefficient of skin friction $\tilde{C}_f$ and Nusselt number $\widetilde{N}_u$ are defined as:

$$\tilde{C}_f = \frac{l^2}{\tilde{x}\,(1-\bar{\alpha}\tilde{t}) Re_{\tilde{x}} C_f} = B_1 (1-\omega)^{2.5} \frac{d^2 g(1)}{d\xi^2}, \tag{2.7a}$$

$$\widetilde{N} = \sqrt{1-\bar{\alpha}\tilde{t}}\, N_u = -\,B_3\,(1+\,N_r)\frac{d\theta}{d\xi}, \tag{2.7b}$$

where $C_f = \frac{\tilde{\mu}_{nf}\,(\frac{\partial \tilde{T}}{\partial \tilde{t}})_{\tilde{y}=\tilde{h}(\tilde{t})}}{\tilde{\rho}_{nf}\, v_w^2}$, $N_u = \frac{l\,(\frac{\partial \tilde{T}}{\partial \tilde{t}})_{\tilde{y}=\tilde{h}(\tilde{t})}}{\tilde{k}_{nf}\tilde{T}_H}$,

**3. The Basic Steps of the New Approach Method (NAM)**

The important foundation for constructing the analytical approximate solution is assumed the coefficient of power series for this solution. Thus, it can be calculated by differential methods. Clarify the calculation of these coefficients and derivation of the NAM, we point to the details of a NAM in four steps as follows:

**The first step:** Assume the ordinary differential equation in the following :

$$G\left(g(\xi), \frac{dg(\xi)}{d\xi}, \frac{d^2 g(\xi)}{d\xi^2}, \frac{d^3 g(\xi)}{d\xi^3}, \dots, \frac{d^{(n-1)} g(\xi)}{d\xi^{(n-1)}}, \frac{d^{(n)} g(\xi)}{d\xi^{(n)}}\right). \tag{3.1}$$

Rewriting the Equation (3.1), then it becomes

$$\frac{d^{(n)} g(\xi)}{d\xi^{(n)}} = G\left(g(\xi), \frac{dg(\xi)}{d\xi}, \frac{d^2 g(\xi)}{d\xi^2}, \frac{d^3 g(\xi)}{d\xi^3}, \dots, \frac{d^{(n-1)} g(\xi)}{d\xi^{(n-1)}}\right), \tag{3.2}$$

Where, $G$ is a function of $g(\xi)$ with its derivatives, $g(\xi)$ is an unbeknown function, $\xi$ denotes the independent variable. So, the integrating of Equation (3.2) n –times with respect to $\xi$ on $[0, \xi]$, this yields

$$g(\xi) = \sum_{j=1}^{n} \frac{\xi^{j-1}}{(j-1)!} g^{(j-1)}(0) + L^{-1} K[g(\xi)], \tag{3.3}$$

where,

$$K[g(\xi)] = G\left(g(\xi), \frac{dg(\xi)}{d\xi}, \frac{d^2 g(\xi)}{d\xi^2}, \frac{d^3 g(\xi)}{d\xi^3}, \dots, \frac{d^{(n-1)} g(\xi)}{d\xi^{(n-1)}}\right), L^{-1}(.) = \int_0^{\xi} \dots \int_0^{\xi} (.)(d\xi)^n,$$

**The second steps:** Suppose that

$$k[g(\xi)] = \sum_{m=1}^{\infty} \frac{d^{(m-1)} K[g_0(\xi)]}{d\xi^{(m-1)}}, \tag{3. 4}$$

rewriting the Equation (3.4) as follows

$$K[g(\xi)] = K[g_0(\xi)] + k[g_0(\xi)] + K''[g_0(\xi)] + K'''[g_0(\xi)] + \cdots, \tag{3.5}$$

substituting Equation(3.5) in Equation(3.3), we get

$$g(\xi) = g_0(\xi) + g_1(\xi) + g_2(\xi) + g_3(\xi) + \cdots, \tag{3.6}$$

$$g(0) = \sum_{j=1}^{n} \frac{\xi^{j-1}}{(j-1)!} g^{(j-1)}(0), \;\; g_1(\xi) = L^{-1} K[g_0(\xi)], \;\; g_2(\xi) = L^{-1} k[g_0(\xi)],$$

$$g_3(\xi) = L^{-1} K'''[g_0(\xi)], \;\; g_4(\xi) = L^{-1} K''''[g_0(\xi)], \dots, \tag{3.7}$$

**The three steps:** The derivative of $k$ with respect to $\xi$ which is the important part of the NAM. Start calculating $K[g(\xi)]$, $K[g(\xi)]$, $K[g(\xi)]$, ...,

$$K[g(\xi)] = G\left(g(\xi), \frac{dg(\xi)}{d\xi}, \frac{d^2 g(\xi)}{d\xi^2}, \frac{d^3 g(\xi)}{d\xi^3}, \dots, \frac{d^{(n-1)} g(\xi)}{d\xi^{(n-1)}}\right), \tag{3.8}$$

$$K'[g(\xi)] = \sum_{s_1=1}^{n} K_{g^{(s_1-1)}} . (g_\xi)^{(s_1-1)}, \tag{3.9}$$

$K''[g(\xi)] = \sum_{s_2=1}^{n}\sum_{s_1=1}^{n} K_{g^{(s_1-1)}g^{(s_2-1)}}.(g_\xi)^{(s_1-1)}.(g_\xi)^{(s_2-1)} +$
$\sum_{s_1=1}^{n} K_{g^{(s_1-1)}}.(g_{\xi\xi})^{(s_1-1)},$ (3.10)

$K''[g(\xi)] = \sum_{s_2=1}^{n}\sum_{s_1=1}^{n} K_{g^{(s_1-1)}g^{(s_2-1)}}.(g_\xi)^{(s_1-1)}.(g_{\xi\xi})^{(s_2-1)}, + \sum_{s_1=1}^{n} K_{g^{(s_1-1)}}.(g_{\xi\xi\xi})^{(s_1-1)}$
$+ \sum_{s_3=1}^{n}\sum_{s_2=1}^{n}\sum_{s_1=1}^{n} K_{g^{(s_1-1)}g^{(s_2-1)}g^{(s_3-1)}} (g_\xi)^{(s_1-1)}.(g_\xi)^{(s_2-1)}.(g_\xi)^{(s_3-1)}$ (3.11)

⋮

Note that, the mixed of derivatives are identical due to the solution of $g$ and the operator of $K$ are analytic functions. The derivative of $g$ is unknown, so we propose the following hypothesis

$g_\xi = g_1 = L^{-1}K[g_0(\xi)], \quad g_{\xi\xi} = g_2 = L^{-1}K'[g_0(\xi)],$
$g_{\xi\xi\xi} = g_3 = L^{-1}K''[g_0(\xi)], \quad g_{\xi\xi\xi\xi} = g_4 = L^{-1}K'''[g_0(\xi)],\ldots$ (3.12)

Therefore, Equations (3.8) - (3.11) are evaluated by

$K[g_0(\xi)] = G\left(g_0(\xi), \frac{dg_0(\xi)}{d\xi}, \frac{d^2g_0(\xi)}{d\xi^2}, \frac{d^3g_0(\xi)}{d\xi^3}, \ldots, \frac{d^{(n-1)}g_0(\xi)}{d\xi^{(n-1)}}\right),$ ()

$K'[g_0(\xi)] = \sum_{s_1=1}^{n} K_{g_0^{(s_1-1)}}.(g_1)^{(s_1-1)},$ (3.14)

$K''[g_0(\xi)] = \sum_{s_2=1}^{n}\sum_{s_1=1}^{n} K_{g_0^{(s_1-1)}g_0^{(s_2-1)}}.(g_1)^{(s_1-1)}.(g_1)^{(s_2-1)} +$
$\sum_{i=1}^{n} K_{g_0^{(s_1-1)}}.(g_2)^{(s_1-1)},$ (3.15)

$K''[g_0(\xi)] = 3.\sum_{j=1}^{n}\sum_{i=1}^{n} K_{g_0^{(s_1-1)}g_0^{(s_2-1)}}.(g_1)^{(s_1-1)}.(g_2)^{(s_2-1)}, + \sum_{i=1}^{n} K_{g_0^{(s_1-1)}}.(g_3)^{(s_1-1)}$
$+ \sum_{s_3=1}^{n}\sum_{s_2=1}^{n}\sum_{s_1=1}^{n} K_{g_0^{(s_1-1)}g_0^{(s_2-1)}g_0^{(s_3-1)}} (g_1)^{(s_1-1)}.(g_1)^{(s_2-1)}.(g_1)^{(s_3-1)},$ (3.16)

⋮

**The four steps:** This step involves making up Equations (3.13)-(3.16) in Equation (3.6), by substitution, we get the required analytical solution to the Equation (3.1).

## 4. The application of NAM for heat transfer in unsteady MHD on flow in the porous medium

In the previous section that described NAM, this method is implemented for solving the system of ordinary differential equations (2.5a) and (2.5b) due to finding the analytical approximate solution $g(\xi)$ and $\theta(\xi)$, The required information is as follows:

From step(1), by integrating Equation (2.5a)4-times and Equation (2.5b)2-times with respect to $\xi$ on $[0, \xi]$, we have

$g(\xi) = g(0) + g'(0)\xi + g''(0)\frac{\xi^2}{2!} + g'''(0)\frac{\xi^3}{3!} + L^{-1}[SB_1(1-\omega)^{0.5}\left(\xi\frac{d^3g}{d\xi^3} + 3\frac{d^2g}{d\xi^2} +\right.$
$\left.\frac{dg}{d\xi}\frac{d^2g}{d\xi^2} - g\frac{d^3g}{d\xi^3}\right) + (\gamma + M)\frac{d^2g}{d\xi^2}$ (4.1a)

$\theta(\xi) = \theta(0) + \theta'(0)\xi + L^{-1}[\frac{-1}{(1+N_r)}\frac{B_2}{B_3}P_rS\left(g\frac{d\theta}{d\xi} - \xi\frac{d\theta}{d\xi}\right)$
$-\frac{1}{(1+N_r)}\frac{P_rE_c}{B_3(1-\omega)^{2.5}}\left[\left(\frac{d^2g}{d\xi^2}\right)^2 + 4\delta^2\left(\frac{dg}{d\xi}\right)^2\right]],$ (4.1b)

rewrite the Equations(4.1a) and (4.1b) as follows:

$$g(\xi) = J_1 + J_2\xi + J_3\frac{\xi^2}{2!} + J_4\frac{3}{3!} + L_1^{-1}K_1[g(\xi)], \tag{4.2a}$$

$$\theta(\xi) = F_1 + F_2\xi + L_2^{-1}K_2[\theta(\xi)], \tag{4.2b}$$

which,

$J_1 = g(0), \ J_2 = g'(0), \ J_3 = g''(0), \ J_4 = g'''(0),$
$F_1 = \theta(0), \ F_1 = \theta'(0),$
$K_1[g] = SB_1(1-\omega)^{0.5}\left(\xi\frac{d^3g}{d\xi^3} + 3\frac{d^2g}{d\xi^2} + \frac{dg}{d\xi}\frac{d^2g}{d\xi^2} - g\frac{d^3g}{d\xi^3}\right) + (\gamma + M)\frac{d^2g}{d\xi^2},$
$K_2[\theta(\xi)] = \frac{-1}{(1+N_r)}\frac{B_2}{B_3}P_rS\left(g\frac{d\theta}{d\xi} - \xi\frac{d\theta}{d\xi}\right) - \frac{1}{(1+N_r)}\frac{P_rE_c}{B_3(1-\omega)^{2.5}}\left[\left(\frac{d^2g}{d\xi^2}\right)^2 + 4\delta^2\left(\frac{dg}{d\xi}\right)^2\right],$

and $L_2^{-1}=\int_0^\xi\int_0^\xi\int_0^\xi\int_0^\xi(.)(d\xi)^4$, $L_2^{-1}=\int_0^\xi\int_0^\xi(.)(d\xi)^2$,
from the boundary conditions ( 4.2a) and (4.2b), we get

$$g(\xi)=J_2\xi+J_4\frac{\xi^3}{3!}+L_1^{-1}K_1[g(\xi)], \tag{4.3a}$$
$$\theta(\xi)=F_1+L_2^{-1}K_2[\theta(\xi)], \tag{4.3b}$$

from step(2), we have

$$g_0=e_w+J_2\xi+J_4\frac{\xi^3}{3!},\quad g_1=L_1^{-1}K_1[g_0(\xi)],\quad g_2=L_1^{-1}K_1'[g_0(\xi)],\ldots, \tag{4.5a}$$
$$\theta_0=F_1,\quad \theta_1=L_2^{-1}K_2[\theta_0(\xi)],\quad \theta_2=L_2^{-1}K_2[\theta_0(\xi)],\ldots, \tag{4.5b}$$

and the analytical solutions are

$$g(\xi)=g_0+g_1+g_2+\cdots, \tag{4.6a}$$
$$\theta(\xi)=\theta_0+\theta_1+\theta_2+\cdots, \tag{4.6b}$$

from step(3), it yields

$$K_1[g]=SB_1(1-\omega)^{0.5}\left(\xi\frac{d^3g}{d\xi^3}+3\frac{d^2g}{d\xi^2}+\frac{dg}{d\xi}\frac{d^2g}{d\xi^2}-g\frac{d^3g}{d\xi^3}\right)+(\gamma+M)\frac{d^2g}{d\xi^2}, \tag{4.7a}$$
$$K_2[\theta(\xi)]=\frac{-1}{(1+N_r)}\frac{B_2}{B_3}P_rS\left(g\frac{d\theta}{d\xi}-\xi\frac{d\theta}{d\xi}\right)-\frac{1}{(1+N_r)}\frac{P_rE_c}{B_3(1-\omega)^{2.5}}\left[\left(\frac{d^2g}{d\xi^2}\right)^2+4\delta^2\left(\frac{dg}{d\xi}\right)^2\right], \tag{4.7b}$$
$$K_1'[g(\xi)]=\sum_{s_1=1}^4K_{1g^{(s_1-1)}}.(g_\xi)^{(s_1-1)}, \tag{4.8a}$$
$$K_2'[\theta(\xi)]=\sum_{s_1=1}^3K_{2g^{(s_1-1)}}.(g_\xi)^{(s_1-1)}+K_{2\theta'}.(\theta_\xi)', \tag{4.8b}$$
$$K_1''[g(\xi)]=\sum_{s_2=1}^4\sum_{s_1=1}^4K_{1g^{(s_1-1)}g^{(s_2-1)}}.\left(g_\xi\right)^{(s_1-1)}.\left(g_\xi\right)^{(s_2-1)} +\sum_{s_1=1}^4K_{1g^{(s_1-1)}}.(g_{\xi\xi})^{(s_1-1)}, \tag{4.9a}$$
$$K_2''[\theta(\xi)]=\sum_{s_2=1}^3\sum_{s_1=1}^3K_{2g^{(s_1-1)}g^{(s_2-1)}}.\left(g_\xi\right)^{(s_1-1)}.\left(g_\xi\right)^{(s_2-1)}$$
$$\sum_{s_1=1}^3K_{2g^{(s_1-1)}}.\left(g_{\xi\xi}\right)^{(s_1-1)}+K_{2\theta'\theta'}.\left(\theta_\xi\right)'^2+K_{2\theta'}.\left(\theta_{\xi\xi}\right)'$$
$$+K_{2g'\theta'}.\left(\theta_\xi\right)'.\left(g_\xi\right)'+K_{2g''\theta'}.(\theta_\xi)'.\left(g_\xi\right)'', \tag{4.9b}$$
$$K_1''[g(\xi)]=3.\sum_{s_2=1}^n\sum_{s_1=1}^nK_{g^{(s_1-1)}g^{(s_2-1)}}.\left(g_\xi\right)^{(s_1-1)}.\left(g_{\xi\xi}\right)^{(s_2-1)}+$$
$$\sum_{s_1=1}^nK_{g^{(s_1-1)}}.(g_{\xi\xi\xi})^{(s_1-1)}+$$
$$\sum_{s_2=1}^n\sum_{s_1=1}^nK_{g^{(s_1-1)}g^{(s_2-1)}g^{(s_1-1)}}\ (g_\xi)^{(i-1)}.(g_\xi)^{(j-1)}.(g_\xi)^{(k-1)}, \tag{4.10a}$$
$$K_2''[\theta(\xi)]=3.\sum_{s_2=1}^n\sum_{s_1=1}^nK_{2g^{(s_1-1)}g^{(s_2-1)}}.\left(g_\xi\right)^{(s_1-1)}.\left(g_{\xi\xi}\right)^{(s_2-1)}$$
$$+\ \sum_{s_1=1}^nK_{2g^{(s_1-1)}}.(g_{\xi\xi\xi})^{(s_1-1)}+$$
$$\sum_{s_3=1}^n\sum_{s_2=1}^n\sum_{s_1=1}^nK_{2g^{(s_1-1)}g^{(s_2-1)}g^{(s_3-1)}}\ (g_\xi)^{(s_1-1)}.(g_\xi)^{(s_2-1)}.(g_\xi)^{(s_3-1)}+$$
$$3.K_{2gg\theta'}.(\theta_\xi)'.(g_\xi)^2+6.K_{2gg'\theta'}.(\theta_\xi)'.(g_\xi)'.\left(g_\xi\right)+4.K_{2gg''\theta'}.(\theta_\xi)'.(g_\xi)''.\left(g_\xi\right)+$$
$$3.K_{2g\theta'\theta'}.(\theta_\xi)'^2.\left(g_\xi\right), \tag{4.10b}$$

Therefore, we propose the hypothesis as follows

$$g_\xi=g_1=L^{-1}K_1[g_0(\xi)],\qquad g_{\xi\xi}=g_2=L^{-1}K_1'[g_0(\xi)], \tag{4.11a}$$
$$\theta_\xi=\theta_1=L^{-1}K_1[\theta_0(\xi)],\qquad \theta_{\xi\xi}=\theta_2=L^{-1}K_1'[\theta_0(\xi)], \tag{4.11b}$$

Now, we have to extract the first derivatives of K in the following

$k_{1g_0}=SB_1(1-\omega)^{2.5}g_0''',k_{1g_0g_0}=k_{1g_0g_0'}=0,k_{1g_0g_0'''}=SB_1(1-\omega)^{2.5}$,
$k_{1g_0g_0g_0}=k_{1g_0g_0g_0'}=k_{1g_0g_0'g_0'}=k_{1g_0g_0'g_0'}=k_{1g_0g_0''g_0''}=k_{1g_0g_0'''g_0'''}=0$,
$k_{1g_0'}=SB_1(1-\omega)^{2.5}(3+g_0'''),k_{1g_0g_0'}=k_{1g_0'g_0'''}=0,k_{1g_0'g_0''}=SB_1(1-\omega)^{2.5}$,
$k_{1g_0g_0g_0'}=k_{1g_0g_0'g_0'}=k_{1g_0'g_0'g_0'}=k_{1g_0'g_0'''g_0'}=k_{1g_0'g_0''g_0''}=k_{1g_0'g_0'''g_0'''}=0$,

$k_{1g_0''} = SB_1(1-\omega)^{2.5}(3+g_0''') + (M+\gamma), k_{1g_0''g_0'''} = 0, k_{1g_0''g_0'} = SB_1(1-\omega)^{2.5}$,
$k_{1g_0''g_0g_0'} = k_{1g_0''g_0'g_0'} = k_{1g_0''g_0'g_0'} = k_{1g_0''g_0'''g_0'} = k_{1g_0''g_0''g_0''} = k_{1g_0''g_0'''g_0'''} = 0$,
$k_{1g_0'''} = SB_1(1-\omega)^{2.5}(\xi - g_0), k_{1g_0'''g_0''} = 0, k_{1g_0'''g_0} = SB_1(1-\omega)^{2.5}$,
$k_{1g_0'''g_0g_0'} = k_{1g_0'''g_0'g_0'} = k_{1g_0'''g_0'g_0'} = k_{1g_0'''g_0'''g_0'} = k_{1g_0'''g_0''g_0''} = k_{1g_0'''g_0'''g_0'''} = 0$, (4.12a)
$K_{2g_0} = \frac{-P_rSB_2}{B_3(1-\omega)^{2.5}(1+N_r)}\theta_0', k_{2g_0g_0'} = k_{2g_0g_0''} = k_{2g_0g_0} = 0, K_{2g_0\theta_0'} = \frac{-P_rSB_2}{B_3(1-\omega)^{2.5}(1+N_r)}$,
$k_{2g_0g_0g_0} = k_{2g_0g_0'g_0} = k_{2g_0g_0'g_0'} = k_{2g_0'g_0'''g_0'} = k_{2g_0g_0''g_0''} = k_{2g_0g_0'''g_0'''} = 0$,
$K_{2g_0'} = \frac{-8\delta^2P_rE_c}{B_3(1-\omega)^{2.5}}g_0', k_{2g_0g_0'} = k_{2g_0'g_0'} = 0, K_{2g_0g_0'} = \frac{-8P_r\delta^2E_c}{B_3(1-\omega)^{2.5}}$,
$k_{2g_0'g_0g_0} = k_{2g_0g_0'g_0'} = k_{2g_0'g_0'g_0'} = k_{2g_0'\theta_0'g_0'} = k_{2g_0'\theta_0'\theta_0'} = k_{2g_0'g_0''g_0'''} = 0$,
$K_{2g_0''} = \frac{-2P_rE_c}{B_3(1-\omega)^{2.5}}g_0'', k_{2g_0''g_0'} = k_{2g_0''g_0''} = 0, K_{2g_0''g_0''} = \frac{-2P_rE_c}{B_3(1-\omega)^{2.5}}$,
$k_{2g_0'g_0\theta_0'} = k_{2g_0g_0''g_0'} = k_{2g_0''g_0''g_0'} = k_{2g_0''\theta_0'g_0'} = k_{2g_0''\theta_0'\theta_0'} = k_{2g_0''g_0''g_0'''} = 0$
$k_{2g_0'g_0\theta_0'} = k_{2\theta_0'g_0''g_0'} = k_{2\theta_0'g_0''g_0'} = k_{2\theta_0'\theta_0'g_0'} = k_{2\theta_0'\theta_0'\theta_0'} = k_{2g_0''g_0''g_0'''} = 0$
$K_{2\theta_0'} = \frac{-P_rSB_2}{B_3(1-\omega)^{2.5}(1+N_r)}(g_0-\xi), g_0', k_{2g_0''\theta_0'} = 0, K_{2\theta_0'g_0} = \frac{-P_rSB_2}{B_3(1-\omega)^{2.5}(1+N_r)}$, (4.12b)

from step(4), substituting Equations in Equations (4.7)-(4.10) in Equation (4.11), we obtain
$g_1 = J_2\xi + \frac{1}{6}J_2\xi^2$,
(4.13a)
$\theta_0 = F_1$, (4.13b)

$$g_2 = -\frac{1}{24}SB_1(1-\omega)^{2.5}e_wJ_4\xi^4 + \frac{1}{5}\left(\frac{1}{6}SB_1(1-\omega)^{2.5} + \frac{1}{24}(\gamma+M)\right)J_4\xi^5 + \frac{1}{2520}SB_1(1-\omega)^{2.5}J_4^2\xi^7, \quad (4.14a)$$

$$\theta_1 = -\frac{P_rE_cB_1}{60B_3(1-\omega)^{2.5}}(120J_2^2\delta^2\xi^2 + (2J_4^2\delta^2 + 20J_2J_4\delta^2 + 5J_4^2)\xi^4), \quad (4.14b)$$

Substituting Equations (4.13) and (4.14) in Equations(4.6a) and (4.6b), respectively. We get the following approximate analytical solutions:

$$g(\xi) = J_2\xi + \frac{1}{6}J_2\xi^2 = -\frac{1}{24}SB_1(1-\omega)^{2.5}e_wJ_4\xi^4 + \frac{1}{5}\left(\frac{1}{6}SB_1(1-\omega)^{2.5} + \frac{1}{24}(\gamma + M)\right)J_4\xi^5 + \frac{1}{2520}SB_1(1-\omega)^{2.5}J_4^2\xi^7 + \cdots, \quad (4.15a)$$

$$\theta(\xi) = F_1 - \frac{P_rE_cB_1}{60B_3(1-\omega)^{2.5}}(120J_2^2\delta^2\xi^2 + (2J_4^2\delta^2 + 20J_2J_4\delta^2 + 5J_4^2)\xi^4) + \cdots. \quad (4.15b)$$

## 5.Results and Discussion

The solution of model heat transfer-Nanofluid flow for parallel plates( porous medium) problem obtained in section (4) by using the new approach is effective. The interest of this section is to explore the influences of numerous values of physical parameters with $N_r, e_w, \gamma$, $M$, $\omega$, $P_r$, $E_c$ and $\delta$ under non-dimension on the curves of the velocity $g'(\xi)$ and temperature $\theta(\xi)$ profiles. To exhibit the convergence of the solutions in the Equations (4.15) obtained by the new approach from Tables (3) and (2) can be observed that the value of $g'(0), g''(0)$ and $\theta(0)$ are fixed at (2- 3) iterations for $e_w > 0$. While these values are fixed at (2-4) iterations for $e_w < 0$. As well as, the convergence of the values $g'(0), g''(0)$ and $\theta(0)$ at 4 iterations for $e_w = 0$. Numerical values for Nusselt number $g''(1)$ are shown in Table (5). The observations explain that the magnitude of $g''(1)$ is increasing profile for increasing of $\gamma$ , $M$ and $\omega$. Besides, the magnitude of $g''(1)$ is observed as an increasing field for decreasing values $e_w$. In Tables (6)-(8), there are compared between the resulting solutions, DTM- Padé method and numerical solutions (RK4th and RKF4-5th ). In these tables, we note that the solutions agree well with each other. In particular, this section focuses on the behaviour of solutions according with $N_r, e_w, \gamma$, $M$, $\omega$, $P_r$, $E_c$ and $\delta$ on the curves of the flow field $g'(\xi)$ and thermal field $\theta(\xi)$ are plotted in Figures (2) - (9). The scenarios of these curves under the proposed physical parameters can be seen, these behaviours are in the following sentences:

- **Figure (2):** This figure depicts the influence of increasing $\gamma$ on the curves of the velocity and temperature profile for fix $\mathrm{M} = \mathrm{N_r} = 2,\ \mathrm{P_r} = 6.2,\ \omega = 0.02,\ \mathrm{S} = 1,\ \delta = E_c = 0.01$ and $\mathrm{e_w} = 0.5$. The graph of the curves $g'(\xi)$ is decreasing with the increase of $\gamma$ to be with the neighbor point in contact for $\xi = 0.5$, and then it becomes in reverse position of increasing the values of the porous medium paramter. The configuration of curves position of $g'(\xi)$ has changed and becomes opposite curves to those in $(0.5,1]$. Furthermore, the decreasing of temperature profile for increasing values of the porous medium parameter is obvious. The thermal field reaches to low level for $\xi = 1$ with a thinner boundary layer while the opposite situation happens for $\xi = 0$, that is thickness boundary layer. Arguably, the velocity increases as a function near the lower plate and boosts near the top plate. It can be also seen that for the constant values of the physical parameters, the flow field increases while the thermal profile decreases.
- **Figures (3)** : The behaviors of the profiles of flow and thermal with increasing value $M$ for fixed $P_r = 6.2,\ \omega = 0.02,\ S = 1,\ \delta = 0.01,\ \gamma = 2,\ E_c = 0.01$ and $e_w = 0.5$. are discussed. The figure for this point shows that the flow field and thermal fields behave quite similarly to the motion of the curves with increasing porosity medium parameter.
- **Figure(4):** Several values of the injection- surjection parameter and the values fixed following $M = 2,\ P_r = 6.2,\ \omega = 0.02,\ S = 1, \delta = 0.01,\ \gamma = N_r = 2,$ and $E_c = 0.01$ lead to a reduction the flow field and thermal field.
- **Figure(5):** The graph cleares that the thermal field when $P_r = 6.2, \omega = 0.02, S = 1, \delta = 0.01, \gamma = 2,\ e_w = 0.5,$ and $E_c$ decreasing with increase in the thermal radiation parameter.
- **Figures (6-9):** From these figures, there are evidents that the temperature profiles are gradually decreasing when $\omega,\ \delta, P_r$ and $E_c$ are increased for $M = 1,\ P_r = 6.2,\ \omega = 0.06,\ S = 1, \delta = 0.01,\ \gamma = N_r = 2,$ and $E_c = 0.01$ .

**Table 2-**The convergence of the values $J_2$, $J_4$ and $F_1$ for $N_r = 1, S = 0.1, P_r = 0.2, E_c = 0.05, M = 0, \omega = 0.01, \delta = 0.1, \gamma = 0.1$.

| | $e_w = 0.4$ | | | $e_w = -0.4$ | | |
|---|---|---|---|---|---|---|
| | $J_2$ | $J_4$ | $F_1$ | $J_2$ | $J_4$ | $F_1$ |
| 1 | 0.8942261 | -1.7391098 | 1.0029690 | 2.0807125 | -3.9438904 | 1.006123 |
| 2 | 0.8941698 | -1.7386838 | 1.0030226 | 2.0801790 | -3.9386535 | 1.006751 |
| 3 | 0.8941698 | -1.7386839 | 1.0030227 | 2.0801742 | -3.9386095 | 1.006753 |
| 4 | 0.8941698 | -1.7386839 | 1.0030227 | 2.0801742 | -3.9386095 | 1.006755 |
| 5 | 0.8941698 | -1.7386839 | 1.0030227 | 2.0801742 | -3.9386095 | 1.006755 |
| 6 | 0.8941698 | -1.7386839 | 1.0030227 | 2.0801742 | -3.9386095 | 1.006755 |
| 7 | 0.8941698 | -1.7386839 | 1.0030227 | 2.0801742 | -3.9386095 | 1.006755 |
| 8 | 0.8941698 | -1.7386839 | 1.0030227 | 2.0801742 | -3.9386095 | 1.006755 |

**Table 3-**The convergence of the values $J_2, J_4$ and $F_1$ for $N_r = 1, S = 0.1, P_r = 0.5, E_c = 0.05, M = 0, \omega = 0.01, \delta = 0.1, \gamma = 0.1$.

| | $e_w = 0$ | | | $e_w = 0.1$ | | |
|---|---|---|---|---|---|---|
| | $J_2$ | $J_4$ | $F_1$ | $J_2$ | $J_4$ | $F_1$ |
| 1 | 1.4882740 | -2.8572435 | 1.0101622 | 1.3399153 | -2.5807108 | 1.00924336 |
| 2 | 1.4880543 | -2.8552623 | 1.0107540 | 1.3397489 | -2.5796447 | 1.00967723 |
| 3 | 1.4880533 | -2.8552623 | 1.0107550 | 1.3397489 | -2.5792598 | 1.00967781 |
| 4 | 1.4880533 | -2.8552623 | 1.0107550 | 1.3397489 | -2.5792598 | 1.00967781 |
| 5 | 1.4880533 | -2.8552623 | 1.0107550 | 1.3397489 | -2.5792598 | 1.00967784 |
| 6 | 1.4880533 | -2.8552623 | 1.0107550 | 1.3397489 | -2.5792598 | 1.00967784 |
| 7 | 1.4880533 | -2.8552623 | 1.0107550 | 1.3397489 | -2.5792598 | 1.00967784 |
| 8 | 1.4880533 | -2.8552623 | 1.0107550 | 1.3397489 | -2.5792598 | 1.00967784 |

**Table 4-**The convergence of the values $J_2$, $J_4$ and $F_1$ for $N_r = 2, S = 0.1, P_r = 0.5, E_c = 0.05, M = 1, \omega = 0.01, \delta = 0.1, \gamma = 0.1$.

| | $e_w = 0$ | | | $e_w = 0.1$ | | |
|---|---|---|---|---|---|---|
| | $J_2$ | $J_4$ | $F_1$ | $J_2$ | $J_4$ | $F_1$ |
| 1 | 1.4675049 | -2.608354 | 1.005782 | 1.321125 | -2.355213 | 1.005348 |
| 2 | 1.4655396 | -2.591264 | 1.006826 | 1.319438 | -2.340666 | 1.006169 |
| 3 | 1.4654874 | -2.590865 | 1.006841 | 1.319396 | -2.340342 | 1.006181 |
| 4 | 1.4654868 | -2.590861 | 1.006859 | 1.319396 | -2.340341 | 1.006194 |
| 5 | 1.4654868 | -2.590861 | 1.006859 | 1.319396 | -2.340341 | 1.006194 |
| 6 | 1.4654868 | -2.590861 | 1.006859 | 1.319396 | -2.340341 | 1.006194 |
| 7 | 1.4654868 | -2.590861 | 1.006859 | 1.319396 | -2.340341 | 1.006194 |

**Table 5-**The values of $-\frac{d^2 g(1)}{d\xi^2}$ for $\delta = 0.01, P_r = 6.2, E_c = 0.01$, and $S = 1$.

| $N_r$ | $\gamma$ | $M$ | $e_w$ | $\omega$ | **RKF4-5th [8]** | **NAM** |
|---|---|---|---|---|---|---|
| 0 | 2 | 2 | 0.5 | 0.02 | 2.0920945932 | 2.2090892252 |
| 1 | 2 | 2 | 0.5 | 0.02 | 2.0920945932 | 2.2090892252 |
| 2 | 2 | 2 | 0.5 | 0.02 | 2.0920945932 | 2.2090892252 |
| 4 | 2 | 2 | 0.5 | 0.02 | 2.0920945932 | 2.2090892252 |
| 2 | 0 | 2 | 0.5 | 0.02 | 1.9438901694 | 1.9431971100 |
| 2 | 1 | 2 | 0.5 | 0.02 | 2.0190028272 | 2.0184921420 |
| 2 | 2 | 2 | 0.5 | 0.02 | 2.0920945932 | 2.0908922520 |
| 2 | 4 | 2 | 0.5 | 0.02 | 2.2306798552 | 2.2477072260 |
| 2 | 2 | 0 | 0.5 | 0.02 | 1.9440334782 | 1.9432212800 |
| 2 | 2 | 1 | 0.5 | 0.02 | 2.0194087546 | 2.0196540460 |
| 2 | 2 | 2 | 0.5 | 0.02 | 2.0920945932 | 2.0928359440 |
| 2 | 2 | 4 | 0.5 | 0.02 | 2.2303732505 | 2.2299315350 |
| 2 | 2 | 8 | 0.5 | 0.02 | 2.4836742559 | 2.4688370370 |
| 2 | 2 | 2 | -0.7 | 0.02 | 7.5702584636 | 7.4734905480 |
| 2 | 2 | 2 | -0.5 | 0.02 | 6.6133062839 | 6.5516150440 |
| 2 | 2 | 2 | -0.2 | 0.02 | 5.2103729244 | 5.1837185500 |
| 2 | 2 | 2 | 0.5 | 0.01 | 2.0826698103 | 2.0814934940 |
| 2 | 2 | 2 | 0.5 | 0.04 | 2.1095910317 | 2.1613913670 |
| 2 | 2 | 2 | 0.5 | 0.06 | 2.1241401910 | 2.1241401910 |

**Table 6-**Comparison of $g(\xi)$ and $\theta(\xi)$ for copper-water for $S = 1, P_r = 6.2, \delta = 0.1, \omega = 0.01, E_c = 0.05,$ and $N_r = M = \gamma = e_w = 0$.

| $\xi$ | DTM[4] | | RKF4-5th [8] | | Present Results | |
|---|---|---|---|---|---|---|
| | $g(\xi)$ | $\theta(\xi)$ | $g(\xi)$ | $\theta(\xi)$ | $g(\xi)$ | $\theta(\xi)$ |
| 0.0 | 0.000000 | 1.229308 | 0.000000 | 1.229159 | 0.000000 | 1.220308 |
| 0.1 | 0.148563 | 1.229151 | 0.148569 | 1.229002 | 0.148563 | 1.229145 |
| 0.2 | 0.294239 | 1.228434 | 0. 294251 | 0.294251 | 0.294239 | 1.228398 |
| 0.3 | 0.434131 | 1.226408 | 0.434147 | 1.226260 | 0.434131 | 1.226291 |
| 0.4 | 0.565335 | 1.221822 | 0.565335 | 1.221674 | 0.565313 | 1.221521 |
| 0.5 | 0.684856 | 1.212902 | 0.684856 | 1.212757 | 0.684830 | 1.212245 |
| 0.6 | 0.789675 | 1.197333 | 0.789705 | 1.197193 | 0.789675 | 1.196057 |
| 0.7 | 0.876784 | 1.172209 | 0.876817 | 1.720792 | 0.876784 | 1.722223 |
| 0.8 | 0.943027 | 1.133972 | 0.943063 | 1.133386 | 0.943027 | 1.130171 |
| 0.9 | 0.985197 | 1.078309 | 0.985234 | 1.078224 | 0.985197 | 1.072259 |
| 1.0 | 1.000000 | 1.000000 | 1.000038 | 0.999950 | 1.000000 | 1.000000 |

**Table 7-**Comparison between and Rk4th for $N_r = 1, S = 0.1, P_r = 0.01, E_c = 0.01,$ $M = 0, \omega = 0.01, \delta = 0.1, \gamma = 0.1, e_w = 0$.

| $\xi$ | $g(\xi)$ | RK4th | Relative Error |
|---|---|---|---|
| 0.0 | 0.0000000000 | 0.0000000000 | 0.00000000000000 |
| 0.1 | 0.1483293309 | 0.1483294549 | $8.359769143 \times 10^{-7}$ |
| 0.2 | 0.2937996825 | 0.2937999301 | $8.427503707 \times 10^{-7}$ |
| 0.3 | 0.4335372323 | 0.4335376045 | $8.585183757 \times 10^{-7}$ |
| 0.4 | 0.5646385829 | 0.5646390817 | $8.833961661 \times 10^{-7}$ |
| 0.5 | 0.6841562519 | 0.6841568802 | $9.183566199 \times 10^{-7}$ |
| 0.6 | 0.7890845015 | 0.7890852634 | $9.655483828 \times 10^{-7}$ |
| 0.7 | 0.8763456337 | 0.8763465326 | $1.025735787 \times 10^{-6}$ |
| 0.8 | 0.9427768796 | 0.9427779169 | $1.100259119 \times 10^{-6}$ |
| 0.9 | 0.9851192034 | 0.9851180346 | $1.186455402 \times 10^{-6}$ |

**Table 8-**Comparison between and Rk4th for $N_r = 1, S = 0.1, P_r = 0.01,$ $E_c = 0.01, M = 0, \omega = 0.01, \delta = 0.1, \gamma = 0.1, e_w = 0$.

| $\xi$ | $\theta(\xi)$ | RK4th | Relative Error |
|---|---|---|---|
| 0.0 | 0.0000000000 | 0.000000000 | 0.0000000000000 |
| 0.1 | 1.000065892 | 1.000065914 | $2.199854999 \times 10^{-8}$ |
| 0.2 | 1.000065773 | 1.000065861 | $8.799420461 \times 10^{-8}$ |
| 0.3 | 1.000065435 | 1.000065631 | $1.959871372 \times 10^{-7}$ |
| 0.4 | 1.000064671 | 1.000065011 | $3.399778977 \times 10^{-7}$ |
| 0.5 | 1.000063178 | 1.000063696 | $5.179670076 \times 10^{-7}$ |
| 0.6 | 1.000060560 | 1.000061282 | $7.219557571 \times 10^{-7}$ |
| 0.7 | 1.000056312 | 1.000057259 | $9.469457788 \times 10^{-6}$ |
| 0.8 | 1.000049814 | 1.000051002 | $1.187939413 \times 10^{-6}$ |
| 0.9 | 1.000040317 | 1.000041760 | $1.442939743 \times 10^{-6}$ |

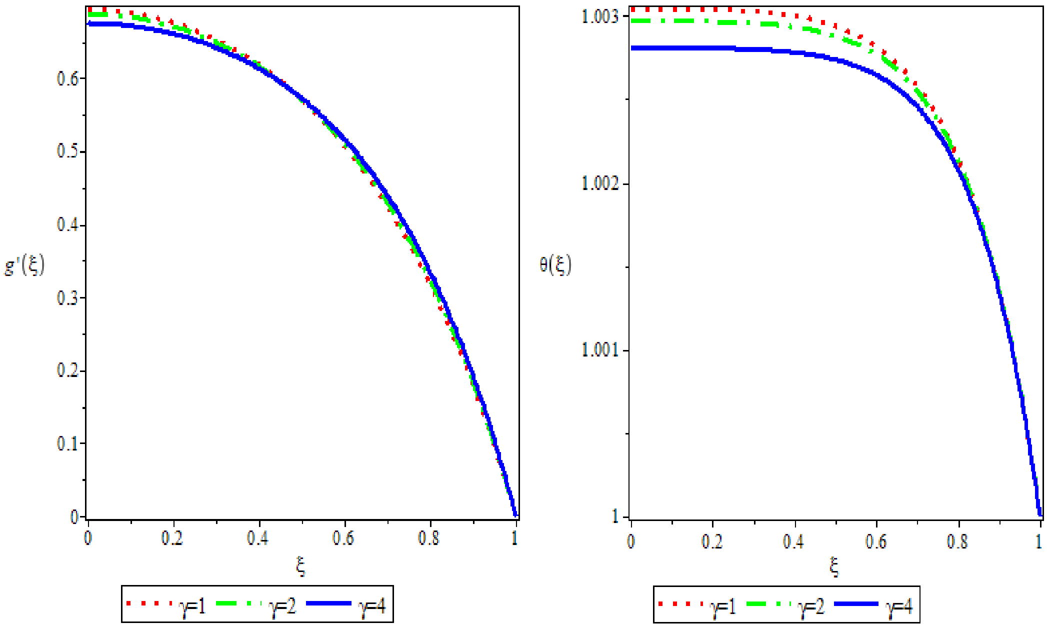


**Figure 2-**The effect of several values of $\gamma$ on $g'(\xi)$ and $\theta(\xi)$.

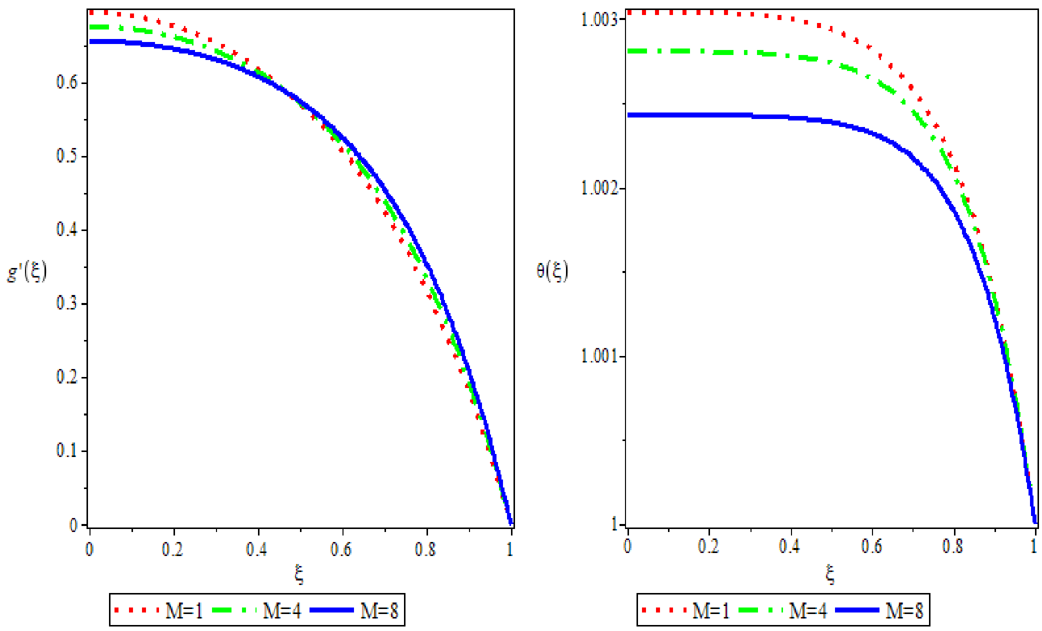


**Figure 3-** The effect of several values of $M$ on $g'(\xi)$ and $\theta(\xi)$.

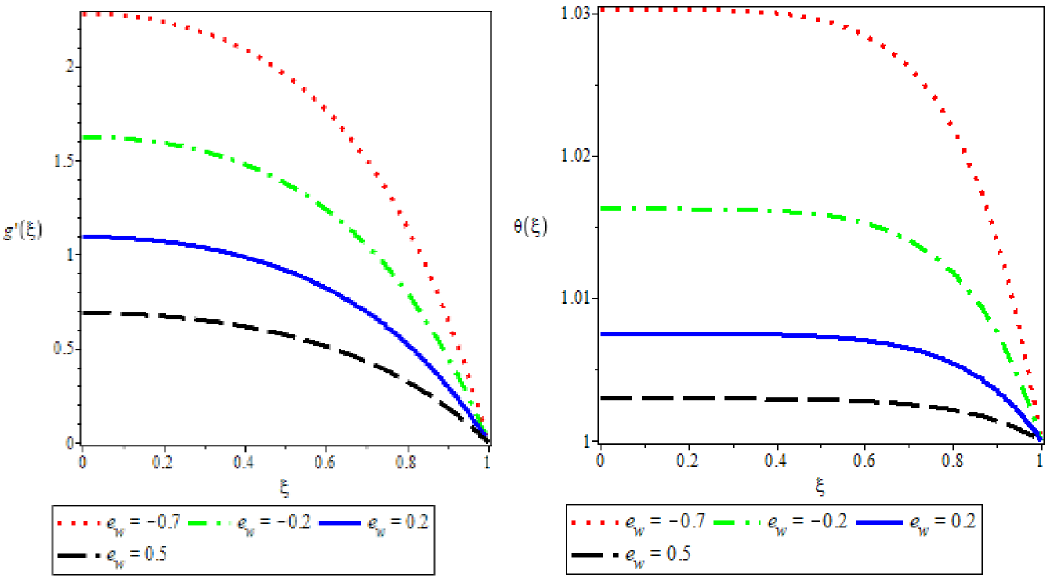


**Figure 4**-The effect of several values of $e_w$ on $g'(\xi)$ and $\theta(\xi)$.

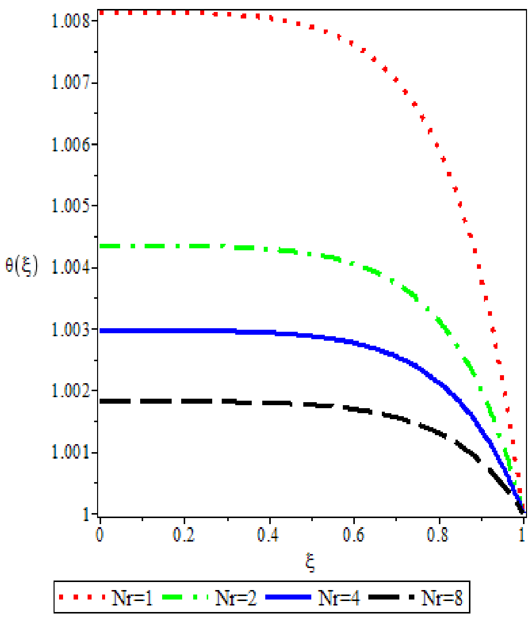


**Figure 5**-The effect of several values of $N_r$ .

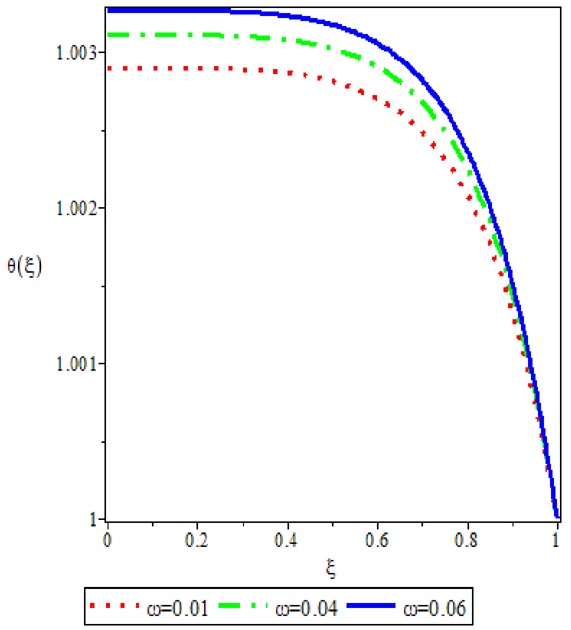


**Figure 6**-The effect of several values of $\omega$ .

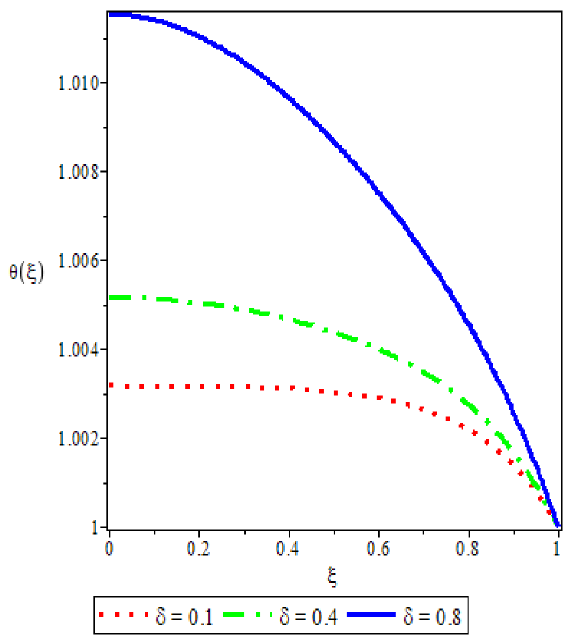


**Figure 7-**The effect of several values of $\delta$ .

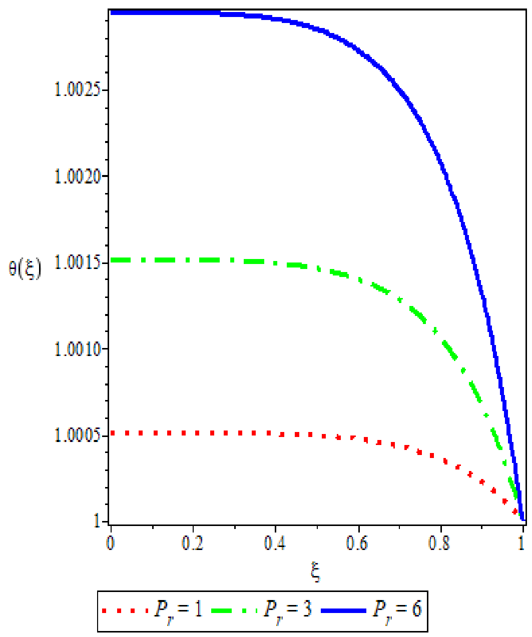


**Figure 8-**The effect of several values of $P_r$ .

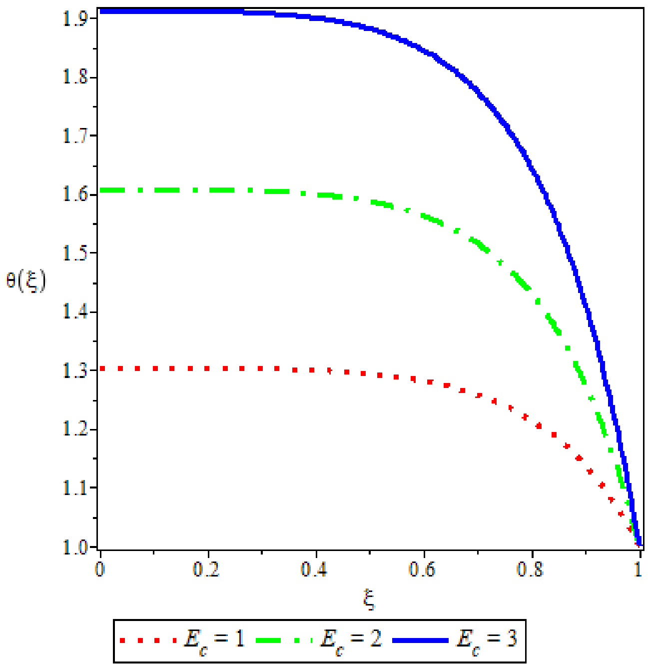


**Figure 9-**The effect of several values of $E_c$ on $\theta(\xi)$.

## 6. Conclusion

In this study, the occurrence of thermal radiation is taken Copper nanofluid particle and water as regular fluid. The effect of various parameters, namely the porous medium parameter, the thermal radiation parameter, the suction-injection parameter, the nanoparticle volume fraction, and the magnetic parameter on MHD of heat transfer nanofluid flow in the porous medium between plates is discussed. The behavior of the dimensionless velocity and temperature curves can be summarized in the following Figure (10) and Figure (11):

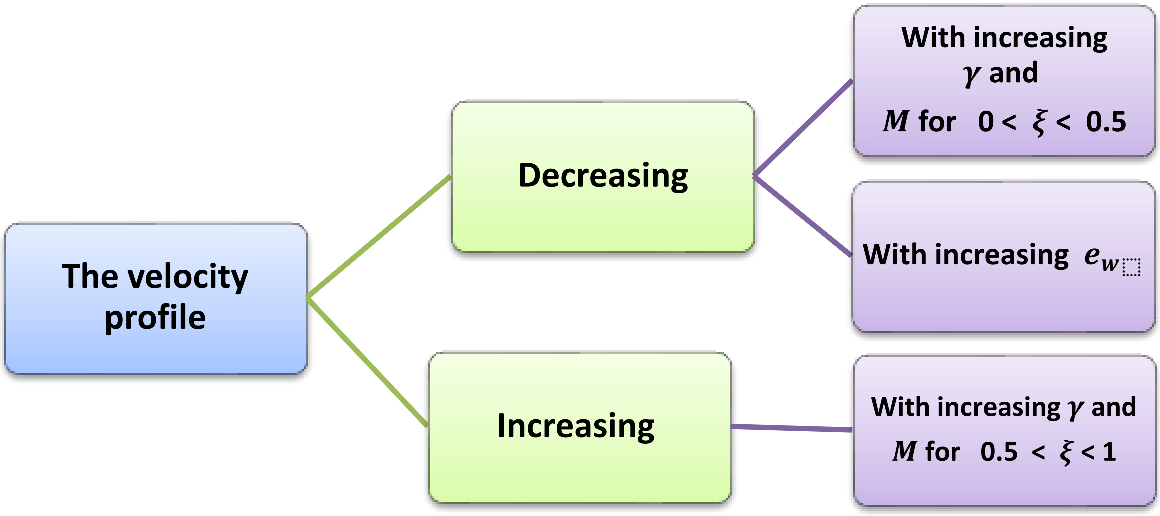


**Figure 10**-The behaviour of the velocity profile

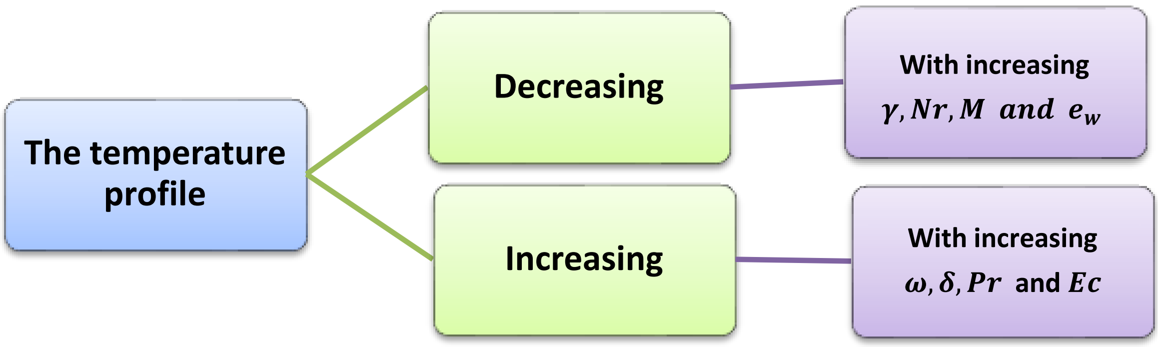


**Figure 11**- The behaviour of the tmperature profile

## References

**[1]** M.Azimi and R.Riazi , "Heat transfer analysis of GO-water nanofluid flow between two parallel disks", *Prop. Power Res*, vol. 4, no. 1, pp. 23-30, 2015.
**[2]** S.Das , A.S.Banu , R.N.Jana , and O.D.Makinde " Entropy analysis on MHD pseudo-plastic nanofluid flow through a vertical porous channel with convective heating" .*Alexandria Eng. J.* , vol.54, no.3, pp. 325-337, 2015.
**[3]** A.Aziz , W.A.Khan and I.Pop " Free convection boundary layer flow past a horizontal flat plate embedded in porous medium filled by nanofluid containing gyrotactic microorganisms".*Int. J. Therm. Sci.* , vol. 56, pp. 48-57,2012.
**[4]** G.Domairry and M.Hatami " Squeezing Cu–water nanofluid flow analysis between parallel plates by DTM-Padé Method ". *J. Mol. Liq.*, vol 193 , pp.37-44, 2014.
**[5]** M.Fakour , D.D.Ganji and M.Abbasi " Scrutiny of underdeveloped nanofluid MHD flow and heat conduction in a channel with porous walls" . *Cas. Stud. Therm. Eng.* , vol.4, pp. 202-214, 2014.
**[6]** T.Groşan , C.Revnic , I.Pop and D.B.Ingham " Free convection heat transfer in a square cavity filled with a porous mediumsaturated by a nanofluid". *Int. J. Heat Mass Transf.*, vol.87, pp.36-41,2015.

**[7]** A.K.Gupta and S.S.Ray "Numerical treatment for investigationof squeezing unsteady nanofluid flow between two parallelplates". *Powd. Technol*., vol.279, pp. 282-289, 2015.

**[8]** K.P.Alok and K.Manoj "Squeezing unsteady MHD Cu-water nanofluid flow between Two Parallel Plates in porous medium with suction/injection ". *Computional and Applied Mathemtics Journal*, vol.4, no.2, pp. 31-42, 2018.

**[9]** W.Ibrahim and B.Shankar "MHD boundary layer flow and heat transfer of a nanofluid past a permeable stretching sheet withvelocity, thermal and solutal slip boundary conditions, Comput. Fluids".vol. 75 pp. 1-10,2019.

**[10]** A.J.A.Al-Saif and A.M.Jasim " A novel algorithm for studying the effects of squeezing flow of a Casson Fluid between parallel plates on magnetic field ". *Journal of Applied Mathematics* 2019.

**[11]** A.J.A.Al-Saif and A.M.Jasim "New analytical study of the effects thermo- diffusion, diffusion-thermo and chemical reaction of viscous fluid on mageto hydrodynamics flow in divergent and convergent channels". *Applied Mathematics*, no.10,pp.268-300, 2019.

**[12]** S.Ding , Z.Lin and C.Wang " Boundary layer for 3D nonlinear parallel pipe flow of nonhomogeneous incompressible Navier-Stokes equations" *Math. Appl. Sci*., pp.43-65., 2020.

**[13]** A.J.A.Al-Saif and A.M.Jasim " Analytical investigation of the MHD Jeffery-Hamel flow through convergent and divergent channel by new scheme" .*Engineering Letters* ,27:3, EL-27-3-28, 2019.

**[14]** A.M.Jasim and A.J.A.Al-Saif " New analytical solution formula for heat transfer of unsteady two-dimensional squeezing flow of a casson fluid between parallel circular plates". *Journal of Advanced Research in Fluid Mechanics and Thermal Sciences*, vol. 64, no.2, pp. 219-243,2019.

**[15]** A.M.Jasim "Analytical approximation of the first grade MHD squeezing fluid flow with slip boundary condition using a new iterative method" *heat transfer*, 1-21,2020.

**[16]** A.M.Jasim " New analytical study for nanofluid between two non-parallel plane palls (Jeffery-Hamel Flow)". *J. Appl. Comput. Mech*, vol.7 , no.1, pp. 213-224,2021.

**[17]** A.M.Jasim "Mean square analytical solution for beta function with second-order random differential equation". *Journal of Physics*, pp.1-13, 2020.

**[18]** A.J.A.Al-Saif and A.M.Jasim " A new analytical-approximate solution for the squeezing flow between two parallel Plates, *Appl. Math. Inf. Sci*. , vol. 13, no.2, pp. 173-182,2019.

**[19]** M.Bousselsal and E.Zaouche "The evolution dam problem for a compressible fluid withnonlinear Darcy's law and Dirichlet boundary condition". *Mtah. Appl. Sci*. vol. 44, pp.66–90, 2021.

**[20]** D.G.S.Al-Khafajy " Radiation and mass transfer effects on MHD oscillatory flow for carreau fluid through an Inclined porous channel" .*Iraqi Journal of Science*, vol.61, no. 6, pp.426-1432,2020..

**[21]** M.A.Rasheed and M.Chlebik **"**Blow-up rate estimates and blow-up set for a system of two heat equations with coupled nonlinear neumann boundary conditions". *Iraqi Journal of Science*, vol. 16, no.1, pp. 147-152, 2020.